# BH4– self-diffusion in liquid LiBH4.

**9 AUTHORS**, INCLUDING:

Pascal Martelli
École Polytechnique Fédérale de Lausanne
**11** PUBLICATIONS **245** CITATIONS

SEE PROFILE

Arndt Remhof
Empa - Swiss Federal Laboratories for Mat…
**136** PUBLICATIONS **2,020** CITATIONS

SEE PROFILE

Philippe Mauron
École Polytechnique Fédérale de Lausanne
**60** PUBLICATIONS **3,002** CITATIONS

SEE PROFILE

# BH4− Self-Diffusion in Liquid LiBH4

**Pascal Martelli,**[*,†,‡] **Arndt Remhof,**[†] **Andreas Borgschulte,**[†] **Philippe Mauron,**[†] **Dirk Wallacher,**[§]
**Ewout Kemner,**[§] **Margarita Russina,**[§] **Flavio Pendolino,**[†] **and Andreas Züttel**[†,‡]

*Empa Swiss Federal Laboratories for Materials Science and Technology, Hydrogen & Energy,*
*8600 Dübendorf, Switzerland, Physics Department, University of Fribourg, 1700 Fribourg, Switzerland, and*
*Department Methods and Instruments, Helmholtz-Zentrum Berlin, Hahn-Meitner Platz 1,*
*14109 Berlin, Germany*

*Received: June 17, 2010; Revised Manuscript Received: August 20, 2010*

The hydrogen dynamics in solid and in liquid LiBH4 was studied by means of incoherent quasielastic neutron scattering. Rotational jump diffusion of the BH4− subunits on the picosecond scale was observed in solid LiBH4. The characteristic time constant is significantly shortened when the system transforms from the low-temperature phase to the high-temperature phase at 383 K. In the molten phase of LiBH4 above 553 K, translational diffusion of the BH4− units is found. The measured diffusion coefficients are in the $10^{-5}$ cm$^2$/s range at temperatures around 700 K, which is in the same order of magnitude as the self-diffusion of liquid lithium or the diffusion of ions in molten alkali halides. The temperature dependence of the diffusion coefficient shows an Arrhenius behavior, with an activation energy of $E_a = 88$ meV and a prefactor of $D_0 = 3.1 \times 10^{-4}$ cm$^2$/s.

## Introduction

Continuous depletion of fossil fuels and growing environmental concerns make energy supply one of the major challenges in the 21st century. The implementation of renewable energy requires new high performance materials for energy conversion, transport, and storage. Thereby, materials for fuel cells and electrolyzer cells, lithium ion batteries, photovoltaics, and materials for hydrogen production and storage are the focus of many research activities worldwide.

Currently, complex hydrides containing BH4− and/or NH2− anions are discussed as high capacity hydrogen storage materials, containing up to 20 mass % of hydrogen.[1−3] Furthermore, some of the Li-based complex hydrides such as $Li_2(BH_4)(NH_2)$ or $Li_4(BH_4)(NH_2)_3$ exhibit fast Li-ion conduction of up to $2 \times 10^{-4}$ S/cm at room temperature,[4] which makes them attractive for solid electrolytes.

Due to its large hydrogen content of 18 mass % $H_2$ and due to its hydrogen sorption reversibility,[5,6] lithium borohydride (LiBH4) is one of the most studied complex hydrides so far. At ambient conditions, it forms an ionic crystal, consisting of Li+ and BH4− ions. It undergoes a structural phase transition from the low-temperature (LT) orthorhombic phase to the high-temperature (HT) hexagonal phase at 383 K.[7−9] Triggered by the phase transition the ion conductivity increases by almost 3 orders of magnitude from $5 \times 10^{-6}$ S/cm to $2 \times 10^{-3}$ S/cm.[10] The hydrogen dynamics in the solid state has been studied extensively by inelastic (INS) and quasielastic neutron scattering (QENS),[9,11] by Raman spectroscopy,[12,13] and by nuclear magnetic resonance spectroscopy.[14,15] While there are rapid localized molecular motions of the BH4− anion, the lateral mobility of individual H atoms is orders of magnitude slower than that of

Li+ cations. Thereby, the main mechanism of hydrogen transport is related to the diffusion of complete BH4− units.[14,16] LiBH4 melts at 553 K and releases considerable amounts of hydrogen from the liquid phase according to the reaction

$$\text{LiBH}_4 \rightarrow \text{LiH} + \text{B} + {}^{3}/_{2}\text{H}_2 \qquad (1)$$

The enthalpy $\Delta H$ and entropy $\Delta S$ of desorption according to eq 1 are determined to be 74 kJ/mol $H_2$ and 115 J/K mol $H_2$, respectively.[6] These thermodynamic parameters relate the equilibrium pressure $p_{eq}$ to the corresponding equilibrium temperature $T_{eq}$ via the van t'Hoff equation:

$$\ln\left(\frac{p_{eq}}{p_0}\right) = \frac{\Delta H}{RT_{eq}} - \frac{\Delta S}{R} \qquad (2)$$

where $p_0$ is the standard pressure of 1013 mbar and $R = 8.31$ J/kmol, the universal gas constant. As long as an applied external hydrogen pressure exceeds the corresponding equilibrium pressure, the decomposition is suppressed and the starting material is stabilized.

The instability of the liquid phase at ambient pressure may be one of the reasons why the dynamics of the liquid state has not been studied so far. In the current study we stabilized the liquid LiBH4 by applying hydrogen pressure of 50 bar, exceeding the equilibrium pressure at 723 K, the maximum temperature in the present experiment, by a factor of 10.[6] We investigated the hydrogen dynamics in the liquid state by means of in situ QENS. Due to the dominating incoherent scattering cross section, QENS is ideally suited to study hydrogen motion in solids and liquids.

## Experimental Methods

QENS measurements were carried out using the time-of-flight (TOF) neutron spectrometer NEAT for cold neutrons located

---

* To whom correspondence should be addressed. E-mail: pascal.martelli@empa.ch.
† Empa Swiss Federal Laboratories for Materials Science and Technology, Hydrogen & Energy.
‡ University of Fribourg.
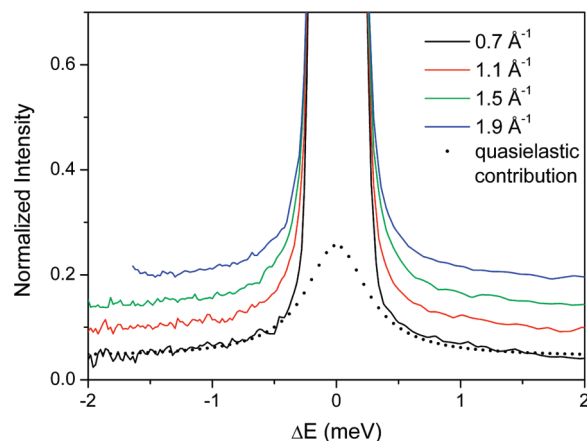§ Helmholtz-Zentrum Berlin.

**Figure 1.** Quasielastic spectra measured at room temperature (low temperature phase). For clarity only the spectra recorded at a momentum transfer of $Q = 0.7$ (black), 1.1 (red), 1.5 (green), and 1.9 Å$^{-1}$ (blue) are shown. The spectra are offset for clarity. Straight lines display the measured data; dotted lines represent the respective quasielastic contribution.
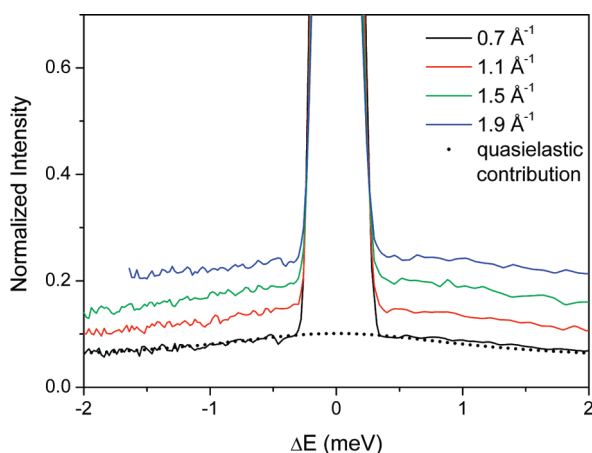


**Figure 2.** Quasielastic spectra measured at 500 K (high temperature phase). For clarity only the spectra recorded at a momentum transfer of $Q = 0.7$ (black), 1.1 (red), 1.5 (green), and 1.9 Å$^{-1}$ (blue) are shown. The spectra are offset for clarity. Straight lines display the measured data; dotted lines represent the respective quasielastic contribution.



**Figure 3.** Quasielastic spectra measured at 573 K (liquid phase). For clarity only the spectra recorded at a momentum transfer of $Q = 0.7$ (black), 1.1 (red), 1.5 (blue), and 1.9 Å$^{-1}$ (green) are shown. The spectra are offset for clarity. Straight lines display the measured data; dotted lines represent the respective quasielastic contribution.



**Figure 4.** Width of the quasielastic contribution measured at 573, 623, 673, and 723 K as a function of momentum transfer $Q$.

at the 10 MW research reactor BERII at the Helmholtzzentrum für Materialien und Energie (HZB) in Berlin, Germany.[17] The incident neutron wavelength was chosen to be 5.1 Å. At the setting used, the energy resolution, $\delta(E)$ was 250 $\mu$eV.

LiBH$_4$ (1.45 g), purchased from Katchem (purity >98%), was used within this experiment. To avoid the strong neutron absorption by $^{10}$B that is present in natural boron, $^{11}$B enriched (99.8%) LiBH$_4$ was used. The sample was handled solely under inert gas conditions (Ar or He).

To minimize absorption and multiple scattering, the sample was filled in a custom-made, double-walled Inconel sample container (30 mm diameter, 1 mm wall spacing) and placed into the high-temperature furnace (HTF), provided by the Dedicated sample environment for in situ gas adsorption (DEGAS) lab of the HZB. The HTF was placed onto the sample stage of the instrument and the sample container was connected to the gas loading system, supplying hydrogen (H$_2$) of 50 bar. During the experiments the temperature of the sample was increased stepwise from room temperature to 723 K. Due to these conditions Inconel has been chosen because of its high mechanical stability at elevated pressure and temperature (contrary to Al) and due to its chemical stability (vanadium
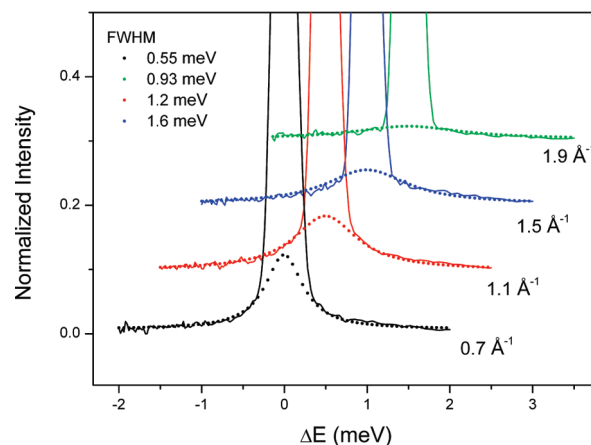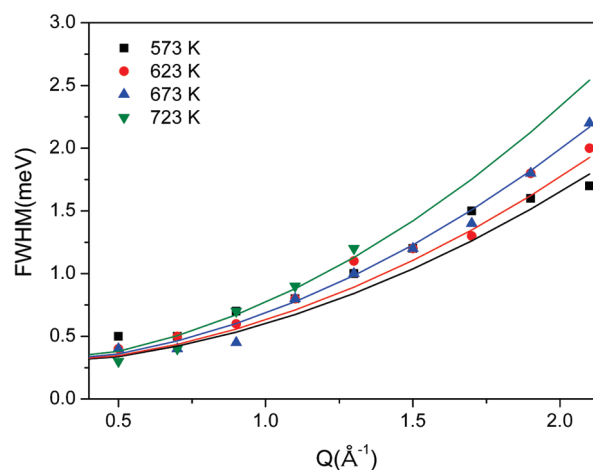
suffers from H embrittlement). The disadvantage of the Inconel sample container is the huge elastic background, which makes an investigation of the elastic contribution, and thereby the evaluation of the elastic incoherent scattering factor (EISF) of the sample impossible.

A single spectrum was recorded within 6 h. The measured TOF data were reduced and binned to quasielastic spectra in the energy range of $\Delta E = \pm 2$ meV and in the momentum transfer range of $Q = 0.5$ to 2.5 A$^{-1}$ with use of the FITMO software package.[18] The instrument resolution of the setting used was determined with a vanadium standard to be $\Gamma_0 = 250$ $\mu$eV.

The quasielastic broadening of each individual spectrum was modeled with a single Lorentzian curve with a width $w_{qe}$ and an integrated area $I_{qe}$. Due to the large elastic contribution of the sample container mentioned before, only the quasielastic component was further evaluated.

Subsequent to the QENS measurements, a fraction of the sample was investigated by X-ray diffraction, to verify the stabilization of the liquid LiBH$_4$ and to exclude the decomposition of LiBH$_4$.

## Results

Figures 1−3 display the quasielastic spectra of LiBH$_4$ measured at room temperature (low-temperature phase), at 500 K (high-temperature phase), and at 573 K (liquid phase),
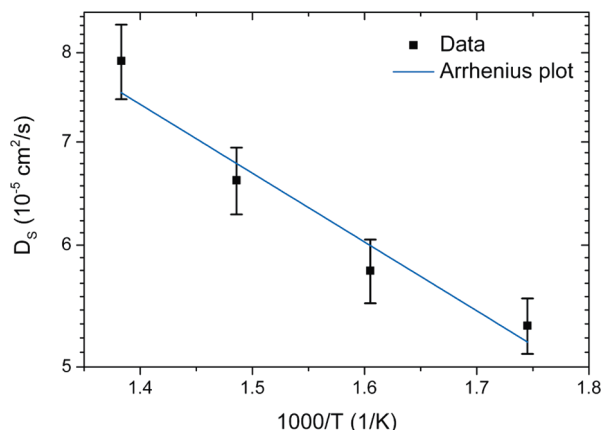
**Figure 5.** Temperature dependence of the self-diffusion coefficient (symbols) and a fit based on the Arrhenius equation (eq 4).

$$\Gamma = \Gamma_0 + \hbar D_s Q^2 \qquad (3)$$

where $\hbar = h/2\pi$ is the reduced Planck constant, $D_s$ is the coefficient of self-diffusion, and $\Gamma_0$ is the instrument resolution of 250 $\mu$eV. All the fits were forced to approach the instrumental resolution at $Q = 0$, according to eq 3. The quasielastic broadening of the spectra recorded at 723 K exceeds the available energy window, especially for $Q$-values above 1.3 Å$^{-1}$. Therefore, the widths of the spectra for $Q > 1.3$ Å$^{-1}$ could not be evaluated. Consequently, these date points were not incorporated in the fit for the diffusion constant at 723 K. The as-calculated diffusion coefficients range from $D_s = 5.3 \times 10^{-5}$ cm$^2$/s at 573 K to $7.9 \times 10^{-5}$ cm$^2$/s at 723 K.

Figure 5 plots the coefficients of self-diffusion over the inverse temperature. The temperature dependence follows roughly the Arrhenius equation:

$$D_s = D_{s,0} \exp(-E_a/kT) \qquad (4)$$

where $D_{s,0}$, the extrapolation to infinite temperature, serves as a prefactor, while $E_a$ is the activation energy and $k$ is the Boltzman constant. Due to the limited amount of data, the uncertainties are rather large. A fit to the data yields $D_{s,0} = 3.1(\pm 1) \times 10^{-4}$ cm$^2$/s and $E_a = 8\ (\pm 15)$ meV.

A comparison of the X-ray diffraction pattern recorded before and after the QENS measurements revealed no sign of decomposition. All the diffraction peaks present after the QENS measurement could be identified as LiBH$_4$ reflections.

## Discussion

Hydrogen dynamics in solid complex hydrides comprises long-range translational diffusion as well as localized motions like vibrations, librations, or rotations.[20,21] The various motions are characterized by their specific length scales and time scales. Within the picosecond range, the time scale accessible of the presently used neutron spectrometer, we
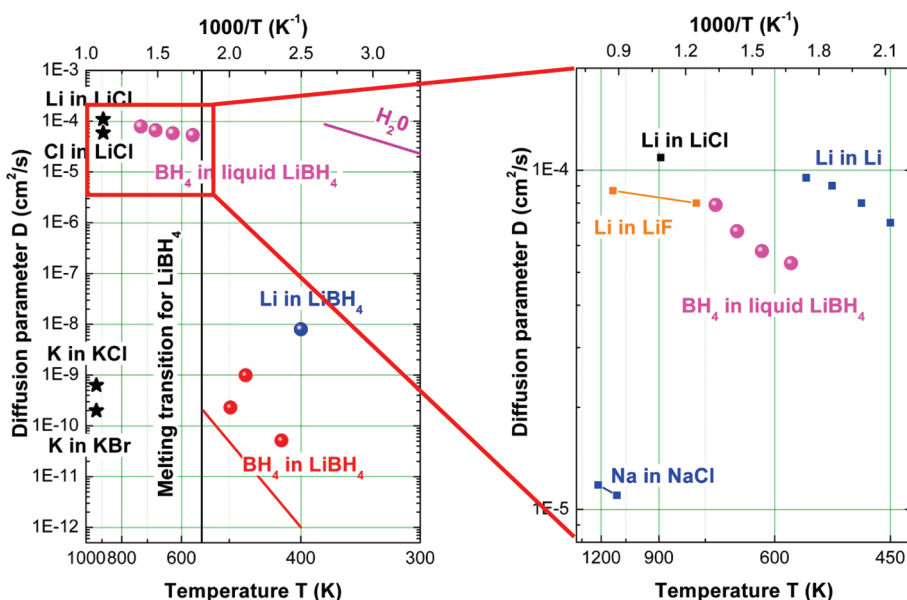
respectively. For clarity only the spectra recorded at a momentum transfer of $Q = 0.7$ (black), 1.1 (red), 1.5 (green), and 1.9 Å$^{-1}$ (blue) are shown. Straight lines display the measured data; dotted lines represent the respective quasielastic contribution.

Within the solid state at a given temperature, the quasielastic broadening is independent of $Q$ as discussed in detail in refs 11 and 19, indicative of a localized hydrogen motion. The impact of the phase transition on the quasielastic broadening is already qualitatively visible when comparing the spectra of the HT phase (Figure 2) with those of the LT phase (Figure 1). In the liquid phase (Figure 3), the quasielastic spectra show a markedly different behavior. Here, the quasielastic signal strongly depends on the momentum transfer, indicative of a lateral diffusion process.

In all cases the quasielastic component can be fitted satisfactorily with a single Lorentzian line shape, as displayed in Figures 1–3. Figure 4 illustrates the $Q$-dependence of the line width of the quasielastic component for different temperatures. The line-width $\Gamma$ increases quadratically with $Q$ and can be expressed as[20]



**Figure 6.** Left: Arrhenius plot of self-diffusivities of BH$_4$ in liquid LiBH$_4$ together with the diffusion of Li and BH$_4$ in solid LiBH$_4$, the diffusion coefficients of Li and Cl in molten LiCl, the diffusion coefficient of K in solid KBr and KCl, and the self-diffusion of liquid water. The vertical line represents the phase transition. This graph is based on citation in ref 27. Right: The right panel compares the Li diffusivities in elemental, liquid Li, and molten salts.

**10120** *J. Phys. Chem. A, Vol. 114, No. 37, 2010*

Martelli et al.

study the rotational jumps of the $BH_4^-$ ions between energetically degenerate positions.[11,19] The orthorhombic to hexagonal phase transition is accompanied by an increase of rotational jump frequency of the $BH_4$ units. This can be clearly seen from the sudden broadening of the quasielastic line above the phase transition temperature. In the high-temperature phase, $LiBH_4$ is a lithium fast-ion conductor, exhibiting a conductivity of more than $10^{-3}$ S/cm. Fast Li-ion conductivity has also been reported from other ionic crystals, with complex anions such as $SO_4^{2-}$. Also these compounds undergo structural phase transitions and similar to $LiBH_4$, the fast ion conductivity and the rotational motion of the anion occur only in the HT phase. Thus the rotation of the anion is believed to support the cation diffusion by the so-called "paddle wheel mechanism".[22,23] However, this interpretation is not without controversy, and the validity of the paddle wheel mechanism is under discussion. Other effects such as a lattice expansion or symmetry changes may be the key factors for both, the enhanced diffusivity of the metal as well as the increase in the rotational motion.[24,25] As $LiBH_4$ contracts during the phase transition,[7] any effect requiring expansion can be excluded. At present it is unclear whether there is a causal connection between the ion conductivity and the $BH_4$ rotation in $LiBH_4$ or not.

In the liquid phase, we clearly see the characteristics of a long-range translational motion. As $LiBH_4$ is an ionic solid, molten $LiBH_4$ consists of $Li^+$ and $BH_4^-$ ions[26] with increased mobility as compared to the solid state. Due to the small inelastic incoherent neutron scattering cross section of lithium as compared to that of hydrogen, the contribution of mobile lithium or boron to the quasielastic spectra of $LiBH_4$ is negligible. The signal is dominated by the hydrogen within the $BH_4^-$ ion. Therefore within the present experiment we determined the diffusion coefficient of the $BH_4^-$ unit within liquid $LiBH_4$.

Figure 6 left compares the measured diffusion coefficient with the reported values of $BH_4^-$ and $Li^+$ in solid $LiBH_4$,[10,27] together with the ionic diffusivity in solid KBr and KCl,[28] with liquid $LiCl$[22] and with the self-diffusion of water.[29] The measured values lie in the $10^{-5}$ cm$^2$/s range (at about 700 K), which is similar to the diffusion coefficients in liquid alkali-halides such as $LiCl$. Upon solidification the diffusion coefficient decreases by about 5 orders of magnitude, which is again analogous to the behavior of the alkali-halides. The right panel compares the Li diffusivities in elemental, liquid Li, and molten salts. (See ref 30 for LiF, ref 25 for NaCl, ref 22 for $LiCl$, and refs 31 and 32 for liquid Li.)

The diffusion coefficient increases with increasing temperature. Applying the Arrhenius law, the activation energy is $E_a$ = 88($\pm$15) meV, which is within the same order of magnitude as the activation energy of the rotational jumps in solid alkali borohydrides.[19] The prefactor might be expressed as $D_{s,0} = d^2\nu$, where $d$ is the average diffusion distance traveled by the migrating particle and $\nu$ is the attempt frequency. Interpreting $d/t$ as the velocity $\nu$ of the diffusing particle, $D_{s,0}$ becomes $D_{s,0} = d\nu$. With $D_{s,0} = 3.1 \times 10^{-4}$ cm$^2$/s and considering $d$ as the interionic distance of about 3 Å or $3 \times 10^{-8}$ cm, the attempt frequency $\nu$ can be estimated to be $3.4 \times 10^{11}$ Hz.

The use of complex hydrides as hydrogen storage materials is hindered by the slow sorption kinetics. One possible barrier is a slow diffusion of species. However, the measured diffusion coefficient in the order of $10^{-5}$ cm$^2$/s is relatively fast when compared to hydrogen diffusion in conventional metal hydrides with fast hydrogen sorption.[33] Therefore the diffusion can be excluded as the rate limiting step for hydrogen sorption in molten $LiBH_4$. The rate limiting step is thus yet due to other mechanisms, such as the formation or the breaking of the B−H bonds, as suggested in ref 34.

Summarizing, we investigated the hydrogen dynamics in solid and liquid $Li^{11}BH_4$ by means of incoherent quasielastic neutron scattering. We successfully stabilized the liquid phase against decomposition up to 723 K (450 °C) by an applied $H_2$ pressure of 50 bar. For the solid phase we can reproduce the experimental results reported in ref 11. In the solid state we observe rotational jump diffusion of the $BH_4$ subunits on the picosecond scale. The phase transition at 383 K is accompanied by a sudden increase of the rotational motion. In the liquid state we observe the translational diffusion of the $BH_4$ ions. The measured diffusion coefficients are in the $10^{-5}$ cm$^2$/s range at temperatures around 700 K, which is in agreement with the self-diffusion in liquid alkali-hydrides. The temperature dependence of the diffusion coefficient can be described by the Arrhenius law, yielding an activation energy of $E_a$ = 88 meV and a prefactor of $D_0 = 3.1 \times 10^{-4}$ cm$^2$/s.

## References and Notes

(1) Züttel, A.; Borgschulte, A.; Orimo, S. *Scr. Mater.* **2007**, *56*, 823–828.

(2) Eberle, U.; Felderhoff, M.; Schüth, F. *Angew. Chem., Int. Ed.* **2009**, *48*, 6608–6630.

(3) Parker, S. F. *Coord. Chem. Rev.* **2010**, *254*, 215.

(4) Matsuo, M.; Remhof, A.; Martelli, P.; et al. *J. Am. Chem. Soc.* **2009**, *131*, 16389–16391.

(5) Orimo, S.; Nakamori, Y.; Kitahara, G.; Miwa, K.; Ohba, N.; Towata, S.; Züttel, A. *Alloys Compd.* **2002**, *404*, 427–430.

(6) Mauron, P.; Buchter, F.; Friedrichs, O.; Remhof, A.; Bielmann, M.; Zwicky, C. N.; Züttel, A. *J. Phys. Chem. B* **2008**, *112*, 906–910.

(7) Soulié, J. P.; Renaudin, G.; Černý, R.; Yvon, K. *J. Alloys Compd.* **2002**, *346*, 200.

(8) Buchter, F.; Łodziana, Z.; Mauron, Ph.; Remhof, A.; Friedrichs, O.; Borgschulte, A.; Züttel, A.; Sheptyakov, D.; Strässle, T.; Ramirez-Cuesta, A. J. *Phys. Rev. B* **2008**, *78*, 094302.

(9) Hartman, M.; Rush, J.; Udovic, T.; Bowman, R.; Hwang, S.-J. *J. Solid State Chem.* **2007**, *180*, 1298–1305.

(10) Matsuo, M.; Nakamori, Y.; Orimo, S.; Maekawa, H.; Takamura, H. *Appl. Phys. Lett.* **2007**, *91*, 224103.

(11) Remhof, A.; Łodziana, F.; Martelli, P.; Friedrichs, O.; Züttel, A.; Skripov, A. V.; Embs, J. P.; Strässle, T. *Phys. Rev. B* **2010**, *81*, 214304.

(12) Hagemann, H.; Gomes, S.; Renaudin, G.; Yvon, K. *J. Alloys Compd.* **2004**, *363*, 129.

(13) Racu, A.-M.; Schoenes, J.; Łodziana, Z.; Borgschulte, A.; Züttel, A. *J. Phys. Chem. A* **2008**, *112*, 9716–9722.

(14) Shane, D. T.; Bowman, R. C., Jr.; Conradi, M. S. *J. Phys. Chem. C* **2009**, *113*, 5039–5042.

(15) Skripov, A. V.; Soloninin, A. V.; Filinchuk, Y.; Chernyshov, D. *J. Phys. Chem. C* **2008**, *112*, 18701.

(16) Gremaud, R.; Łodziana, Z.; Hug, P.; Willenberg, B.; Racu, A.-M.; Schoenes, J.; Ramirez-Cuesta, A. J.; Clark, S. J.; Refson, K.; Züttel, A.; Borgschulte, A. *Phys. Rev. B* **2009**, *80*, 100301.

(17) Lechner, R. E.; Melzer, R.; Fitter, J. *Phys. B* **1996**, *226*, 86–91.

(18) NEAT: http://www.helmholtz-berlin.de/user/neutrons/instrumentation/neutron-instruments/v3/index_en.html.

(19) Remhof, A.; Łodziana, Z.; Buchter, F.; Martelli, P.; Pendolino, F.; Friedrichs, O.; Züttel, A.; Embs, J. P. *J. Phys. Chem. C* **2009**, *113*, 16834–16837.

(20) Embs, J. P.; Jouranyi, F.; Hempelmann, R. *Z. Phys. Chem* **2010**, *224*, 5–32.

(21) Remhof, A.; Gremaud, R.; Buchter, F.; Łodziana, Z.; Embs, J. P.; Ramirez-Cuesta, A. J.; Borgschulte, A.; Züttel, A. *Z. Phys. Chem* **2010**, *224*, 263–278.

(22) Lunden, A.; Mellander, B. E.; Bengtzelius, A.; Ljungmark, H.; Taerneberg, R. *Solid State Ionics* **1986**, *18*, 514.

(23) Lunden, A. Z. *Naturforsch.* **1995**, *50a*, 1067–1076.

(24) Secco, E. A. *Solid State Commun.* **1988**, *66*, 921–923.

(25) Borucka, A. Z.; Bockris, J. O'M.; Kitchener, J. A. *Proc. R. Soc. London* **1957**, *241*, 554–567.

(26) Borgschulte, A.; Züttel, A.; Hug, P.; Racu, A. M.; Schoenes, J. *J. Phys. Chem. A* **2008**, *112*, 4749.

(27) Borgschulte, A.; Gremaud, R.; Łodziana, Z.; Züttel, A. Z. *Phys. Chem. Chem. Phys.* **2010**, *12*, 5061–5066.

(28) Bénière, F.; Bénière, M.; Hari Babu, V.; Reddy, K. V. *J. Phys. Chem. Solids* **1994**, *55*, 595.

(29) Holz, M.; Heil, S. R.; Sacco, A. *Phys. Chem. Chem. Phys.* **2000**, *2*, 4740–4742.

(30) Sarou-Kanian, V.; Rollet, A.-L.; Salanne, M.; Simon, C.; Bessada, C.; Madden, P. A. *Phys. Chem. Chem. Phys.* **2009**, *11*, 11501–11506.

(31) Feinauer, A.; Majer, G.; Seeger, A. *J. Phys.: Condens. Matter* **1994**, *26*, L355–L360.

(32) Murday, J. S.; Cotts, R. M. *J. Chem. Phys.* **1968**, *48*, 4938–4945.

(33) Wipf, H., Ed. *Hydrogen in Metals III: Properties and Applications*, Springer Verlag: Berlin, Germany, 1997.

(34) Friedrichs, O.; Remhof, A.; Borgschulte, A.; Buchter, F.; Orimo, S. I.; Züttel, A. *Phys. Chem. Chem. Phys.* DOI: 10.1039/C0CP00022A. Published Online: July 26, 2010.